Korean J. Chem. Eng., 37(10), 1690-1698 (2020)
DOI: 10.1007/s11814-020-0588-0

pISSN: 0256-1115
eISSN: 1975-7220

Effect of reducibility on the performance of Co-based catalysts for the production of high-calorie synthetic natural gas

Tae Young Kim*,‡, Seong Bin Jo,‡, Chul Ho Lee***, Suk-Hwan Kang****, Joon Woo Kim*****, Soo Chool Lee**,†, and Jae Chang Kim*,†**

*Department of Chemical Engineering, Kyungpook National University, Daegu 41566, Korea
**Research Institute of Advanced Energy Technology, Kyungpook National University, Daegu 41566, Korea
***Korea Institute of Industrial Technology, Ulsan 44413, Korea
****Institute for Advanced Engineering, Yongin 41718, Korea
*****Research Institute of Industrial Science and Technology, Pohang 37673, Korea
(*Received 20 February 2020 • Revised 20 May 2020 • Accepted 27 May 2020*)

Abstract−Co-based catalysts were developed for the production of high-calorie synthetic natural gas. The Co reduction in Al_2O_3- and SiO_2-supported catalysts prepared with different Co loading, and their catalytic properties for high-calorie methanation were investigated. The CO conversion of the Co/SiO_2 catalysts was superior to that of the Co/Al_2O_3 with the same Co loading, due to their better reducibility at 400 °C. The activities of both the Al_2O_3 and SiO_2-supported catalysts increased with Co loading, while the growth of hydrocarbon chains decreased as the Co loading increased. As the reduction temperature increased, crystallite size of Co increased in $10Co/SiO_2$, resulting in decrease of CO conversion and increase of C_{2+} selectivity. The highest CO conversion (98.7%) was obtained over $10Co/SiO_2$ reduced at 400 °C. Moreover, the heating value of the product gas (10,405 kcal/Nm^3) exceeded the standard heating value without requiring a high reduction temperature (700 °C) or a noble metal (Ru).

Keywords: High-calorie Synthetic Natural Gas (HC-SNG), Cobalt, Reducibility, Light Hydrocarbons, Heating Value

INTRODUCTION

Concerns about environmental issues related to global warming are constantly rising, as it is widely accepted that climate change is mainly due to emissions from fossil fuel power plants. Especially, coal-fired power plants emit large amounts of greenhouse gases such as carbon dioxide (CO_2) [1]. Synthetic natural gas (SNG), which is obtained by coal gasification, has attracted increased attention as a clean energy source, as it consists mainly of CH_4 and releases the lowest amount of CO_2 per unit of energy among all fossil fuels [2-4]. Obtaining SNG from coal involves three steps: (1) coal gasification with steam and O_2 to produce CO and H_2 syngas, (2) conversion of the syngas to a mixture of H_2 and CO (3 : 1) by the water gas shift (WGS) reaction ($CO+H_2O=CO_2+H_2$), and (3) CH_4 production from the 3 : 1 H_2/CO syngas ($CO+3H_2=CH_4+H_2O$). The catalysts that are mainly used for CO methanation are based on the group VIII metals Ru, Co, Fe, and Ni. Ni catalysts are more commonly used due to their high catalytic activity for CO methanation and high CH_4 selectivity [5-11]. However, the heating value of CH_4 (9,520 kcal/Nm^3) is below the South Korean standard heating value (10,400 kcal/Nm^3) for power generation [3,4]. Thus, liquefied petroleum gas (LPG), which consists mainly of hydrocarbons that contain three or four carbon atoms, is added to SNG to increase its heating value. Nevertheless, the LPG addition has significant drawbacks, including high cost and supply chain uncertainty. Therefore, to increase the heating value of SNG without the addition of LPG, Co-based catalysts are used to convert syngas to light chain hydrocarbons (C_1-C_4), a reaction known as Fischer-Tropsch synthesis (FTS) [12-15].

Several catalysts have already been reported for the production of high-calorie SNG (HC-SNG), which is comparable to natural gas but includes additional C_2-C_4 hydrocarbons. Inui et al. developed Co-based catalysts on Al_2O_3 supports for the production of HC-SNG with a $10Co\text{-}6Mn\text{-}2Ru/Al_2O_3$ catalyst exhibiting high activity and superior selectivity for C_1-C_4 hydrocarbons [16,17]. Furthermore, Lee et al. reported the effects of the components in Co-Mn-Ru/Al_2O_3 catalysts, demonstrating that the Mn promoter acted as a Lewis acid and enhanced the growth of carbon chains but reduced the catalytic activity at low temperature. In contrast, Ru induced a strong H_2 spillover effect at active sites, resulting in higher activity and a lower Co species reduction temperature, which, however, reduced the C_{2+} hydrocarbon production. Among the catalysts, $10Co\text{-}6Mn\text{-}2.5Ru/Al_2O_3$, reduced at 400 °C, yielded the highest proportion of C_2-C_4 hydrocarbons. Nevertheless, since Ru is a noble metal, its amount should be reduced or replaced to control the material costs. A $20Co\text{-}Mn/Al_2O_3$ catalyst could be used instead, but a higher temperature would be required to reduce the Co sites [3]. Thus, numerous studies on the reducibility of FTS catalysts have been performed using Co-based catalysts. Co-based catalysts on porous supports, such as Al_2O_3, SiO_2, and ZrO_2, have been developed to achieve adequate FTS activity. It was proven that the sup-

†To whom correspondence should be addressed.
E-mail: kjchang@knu.ac.kr, soochool@knu.ac.kr
‡Tae Young Kim and Seong Bin Jo contributed equally to this work.

port can significantly affect the catalytic performance, as the catalytic activity strongly depends on the reducibility of the support material [18-23].

At present, researchers have attempted to enhance the heating value of SNG using Co-based catalysts. However, the effect of metal oxide reducibility between Al_2O_3- and SiO_2-supported Co-based catalysts on the catalytic properties has not been thoroughly investigated for HC-SNG. The aim of this study was to point out the effect of Co reducibility on CO hydrogenation for HC-SNG. More specifically, we aimed to elucidate the influences of the Co loading and the reduction temperature on the catalytic performance, such as CO conversion and hydrocarbon selectivity of Al_2O_3- and SiO_2-supported catalysts.

EXPERIMENTAL

1. Catalyst Preparation

γ-Al_2O_3 and SiO_2 (Davisil 646) with a Brunauer-Emmett-Teller (BET) surface area of 160 and 300 m^2/g, respectively, were obtained from Sigma-Aldrich and used as support materials. The Co-based catalysts were prepared by the wet impregnation of Al_2O_3 and SiO_2 in an ethanolic solution of $Co(NO_3)_2{\cdot}6H_2O$ (Sigma-Aldrich). The mixed samples were stirred for 12 h and then the solvent was removed using a rotary evaporator at 30 °C-40 °C. After impregnation, the samples were dried at 120 °C for 12 h and calcined at 400 °C for 8 h at a heating rate of 5 °C/min. The catalysts were designated as xCo/Al_2O_3 and xCo/SiO_2, where x represents the weight percentage of Co^0 in the catalyst. The Co content in the catalytic powders was determined by inductively coupled plasma-optical emission spectrometric (ICP-OES) chemical analysis, and the results are summarized in Tables 1 and 2.

2. Catalyst Characterization

The textural properties of the catalysts were determined from their N_2 adsorption isotherms, which were obtained using a Micromeritics ASAP 2020 apparatus at −196 °C. Prior to the adsorption measurements, the catalysts were degassed at 200 °C for 5 h. The pore size distribution of each catalyst was determined by the desorption branch of its nitrogen isotherm according to the Barrett-Joyner-Halenda (BJH) method.

To analyze the reducibility of the Co species in the catalysts, H_2 temperature-programmed reduction (H_2-TPR) was performed using a system equipped with a thermal conductivity detector (TCD). At

Table 1. Physicochemical properties of the Al_2O_3-supported Co catalysts

	Co loading[a] (wt%)	BET surface area (m^2/g)	Pore volume (cm^3/g)	Average pore size (nm)	Crystallite size of Co_3O_4[b] (nm)	Dispersion[c] (%)	Degree of reduction[d] (%)	Active metal[e] (10^{-5} mol/g)
Al_2O_3	-	136	0.25	5.5	-	-	-	-
5Co/Al_2O_3	5.2	105	0.19	6.0	8.4	11.4	50.0	2.5
10Co/Al_2O_3	10.9	111	0.18	5.4	8.8	10.9	53.3	5.3
20Co/Al_2O_3	20.1	99	0.15	5.4	11.8	8.1	61.7	8.5
30Co/Al_2O_3	30.2	70	0.12	5.8	21.0	4.5	72.3	8.4

[a]The Co amount was analyzed by ICP-OES.
[b]The Co_3O_4 crystallite sizes were calculated using the Scherrer equation.
[c]The metal dispersion was determined by the equation D%=96/d_p, assuming spherical metal crystallites of uniform diameter d_p with a site density of 14.6 atoms/nm^2.
[d]The degree of reduction was calculated from the weight loss of the catalysts, assuming a stoichiometric reduction of Co_3O_4 to Co using thermogravimetric analysis (TGA).
[e]Active metal content=metal mole×reducibility×dispersion.

Table 2. Physicochemical properties of the SiO_2-supported Co catalysts

	Co loading[a] (wt%)	BET surface area (m^2/g)	Pore volume (cm^3/g)	Average pore size (nm)	Crystallite size of Co_3O_4[b] (nm)	Dispersion[c] (%)	Degree of reduction[d] (%)	Active metal[e] (10^{-5} mol/g)
SiO_2	-	305	1.03	11.0	-	-	-	-
5Co/SiO_2	4.6	280	0.96	11.0	12.2	7.8	87.5	2.6
10Co/SiO_2	9.7	263	0.88	11.0	12.9	7.4	96.0	5.8
20Co/SiO_2	19.5	225	0.74	10.9	14.1	6.8	95.7	10.4
30Co/SiO_2	30.1	180	0.55	10.8	14.7	6.5	99.4	16.5

[a]The Co amount was determined by ICP-OES.
[b]The Co_3O_4 crystallite sizes were calculated using the Scherrer equation.
[c]The metal dispersion was determined by the equation D%=96/d_p, assuming spherical metal crystallites of uniform diameter d_p with a site density of 14.6 atoms/nm^2.
[d]The degree of reduction was calculated from the weight loss of the catalysts, assuming a stoichiometric reduction of Co_3O_4 to Co using thermogravimetric analysis (TGA).
[e]Active metal content=metal mole×reducibility×dispersion.

first, 0.2 g of each catalyst was packed into a quartz reactor and pretreated under N_2 gas flow. The catalysts were then heated at 300 °C for 1 h to remove water and any contaminants, followed by cooling to 100 °C. Finally, for the H_2-TPR measurements, the catalysts were heated to 800 °C at a rate of 10 °C/min in a 10 vol% H_2/N_2 gas mixture with a total flow rate of 100 mL/min.

The crystallite sizes in the calcined and reduced catalysts were determined by X-ray diffraction (XRD) analysis. The XRD patterns from (2θ) 20° to 80° were obtained on a Phillips X'Pert XRD system at the Korea Basic Science Institute in Daegu using Cu Kα radiation (λ=1.5406 Å). Prior to XRD analysis, the catalysts were reduced at 400 °C, 500 °C, and 600 °C for 1 h in a 10% H_2/N_2 gas mixture. The crystallite sizes of the Co species in the calcined catalysts were calculated using the Scherrer equation based on the Co_3O_4 diffraction peak at (2θ) 36.9°.

The degree of reduction was calculated from the weight loss of the catalysts by thermogravimetric analysis (TGA), assuming the stoichiometric reduction of Co_3O_4 to Co. A 20 mg sample was heated in a N_2 flow at 200 °C for 1 h to remove adsorbed water, and the weight loss of each catalyst was calculated under H_2 with a flow rate of 30 mL/min at 400 °C for 1 h.

3. Catalytic Tests

The catalytic hydrogenation of CO was in a fixed-bed stainless steel reactor (O.D. 0.5 in.) using 0.5 g of each catalyst. Before the reaction, each catalyst was reduced by heating at 400 °C, 500 °C, or 600 °C at a heating rate of 10 °C/min. The reactor atmosphere was constant by supplying a 10 vol% H_2/N_2 gas mixture at a flow rate of 100 mL/min for 1 h. After the catalyst reduction, the temperature was reduced to 200 °C under N_2 atmosphere. A $H_2/CO/N_2$ (72 : 24 : 4) gas mixture with a H_2/CO molar ratio of 3.0 was then fed into the reactor at a total gas flow of 50 mL/min. N_2 gas was used as the internal standard. The reactor pressure was increased to 10 bar with the feed gas using a back-pressure regulator. The reactor temperature was then increased from 200 °C to 300 °C at a 10 °C/min rate. To avoid the condensation of the products, the gas transfer lines were maintained at >180 °C. The water vapors and heavy hydrocarbons were collected in a cold trap at 0 °C, followed by the on-line analysis of the outlet gases using a gas chromatograph (6890N, Agilent). CO, H_2, N_2, and CO_2 were analyzed using a Carboxen 1000 column and a TCD. A flame ionization detector (FID) was used for the analysis of the gaseous hydrocarbons after separation on a GS-GASPRO capillary column. The CO conversion and the selectivity for each product were calculated using Eqs. (1), (2), and (3):

$$\text{CO conversion (carbon mol\%)} = \left(1 - \frac{\text{Co in the product gas (mol/min)}}{\text{CO in the feed gas (mol/min)}}\right) \times 100 \quad (1)$$

$$\text{Selectivity for hydrocarbons with carbon number } n \text{ (carbon mol\%)} = \frac{n \times \text{C}_n \text{ hydrocarbon in the product gas (mol/min)}}{(\text{total carbon} - \text{unreacted CO}) \text{ in the product gas (mol/min)}} \times 100 \quad (2)$$

$$\text{Selectivity for carbon dioxide (carbon mol\%)} = \frac{\text{CO}_2 \text{ in the product gas (mol/min)}}{(\text{total carbon} - \text{unreacted CO}) \text{ in the product gas (mol/min)}} \times 100 \quad (3)$$

The heating value of the product gas was calculated using Eq. (4). The heating values of the pure gases were obtained from the NIST Chemistry WebBook [24].

$$\text{Heating value (kcal/Nm}^3) = \Sigma_{n=1}^{4}(x_n \times H_n), \quad (4)$$

where x_n is the volume fraction of C_n hydrocarbons and H_n is the heating value of C_n hydrocarbons (kcal/Nm^3).

RESULTS AND DISCUSSION

1. Co/Al_2O_3 Catalysts for CO Hydrogenation

The BET surface areas, pore volumes, and average pore sizes of the xCo/Al_2O_3 catalysts (x=5, 10, 20, and 30) are summarized in Table 1. Increasing the Co loading (x) from 0 to 30 wt% reduced the BET surface area from 136 to 70 m^2/g and the pore volume from 0.25 to 0.12 cm^3/g. This reduction suggested that the Co species dispersed into the pores of the supports, because the average pore sizes of the catalysts did not vary after impregnation with Co (Supplementary Material, Fig. S1). Thus, the pore structures of the Al_2O_3-supported catalysts remained intact up to a Co loading of 30 wt%.

The catalytic performance of the Al_2O_3-supported Co catalysts at a H_2/CO ratio of 3.0 at 300 °C and 10 bar after reduction at 400 °C was plotted as a function of the Co loading (Fig. 1(a)). The CO conversion increased remarkably from 32.6% to 99.5% as the Co loading increased from 5 to 30 wt%, indicating that the CO

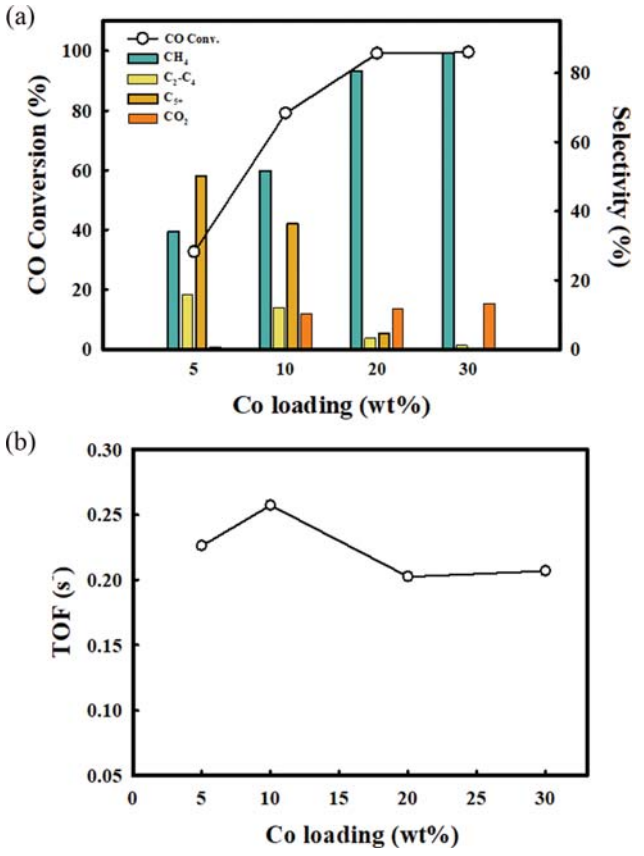

Fig. 1. (a) CO conversion over the xCo/Al_2O_3 catalysts and selectivity for CH_4, C_2-C_4, C_{5+}, and CO_2; (b) TOF of CO conversion as a function of different Co loading.

conversion was highly dependent on the Co loading. The selectivity for CH_4 also increased from 33.8% to 85.8%, while the selectivity for C_2-C_4 and C_{5+} hydrocarbons remarkably decreased from 15.8% to 1.1% and from 49.6% to 0.0%, respectively, as the Co loading increased. In addition, the CO_2 selectivity increased from 0.8% to 13.1% with increasing CO conversion due to an increase in the water gas shift (WGS) reaction ($CO+H_2O=CO_2+H_2$) at high H_2O partial pressures [25]. Thus, although the catalytic activity for CO hydrogenation increased with Co loading, the selectivity for C_2-C_4 hydrocarbons decreased sharply.

The turnover frequency (TOF) value of CO was calculated to express the activity change with Co loading (Fig. 1(b)). The TOF is defined as the number of CO molecules converted into the products per active site per second. Herein, although the CO hydrogenation constantly increased with increasing Co loading, the TOF decreased by increasing the Co loading from 10 to 20 wt%, whereas a slight increase was observed by increasing the Co loading to 30 wt%. But no significant change was identified in the crystallite size of Co by increasing the Co loading from 5 to 10 wt% (Table 1), suggesting that the increased CO conversion over catalysts with higher Co loading was due to the presence of more active Co species. Additionally, the C_1-C_4 space time yield of the $10Co/Al_2O_3$ catalyst improved the catalytic activity much more than other Co loaded catalysts under similar conditions (syngas ratio=3.0, P=10 bar, and T=300 °C) (Fig. S3).

Based on the XRD patterns of the calcined Co/Al_2O_3 catalysts at each Co loading (Fig. 2), diffraction peaks of the Co_3O_4 particles appeared at 31.3°, 36.8°, 45.0°, 59.4°, and 65.4°, while the peak intensities increased with increasing Co loading. Moreover, according to the data of Table 1, the size of the Co_3O_4 crystallites in the Co/Al_2O_3 catalysts increased from 8.4 to 11.8 nm as the Co loading increased. The patterns of the catalysts reduced at 400 °C displayed CoO diffraction peaks at 42.9° and 62.2°, but in the pattern of the $20Co/Al_2O_3$ catalyst an additional Co^0 peak was detected at 44.2°, suggesting that an increase in the size of the Co_3O_4 crystallites enhanced the reducibility of the Co phase. This result was also consistent with a previous report, which indicated that the reducibility of metals depends on the crystallite size [26].

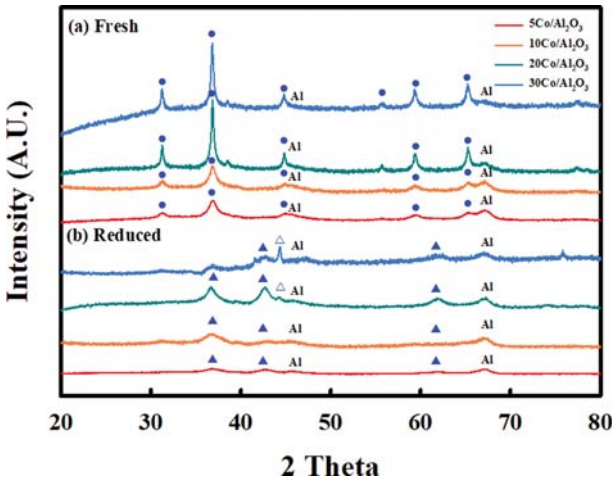

Fig. 2. XRD patterns of the xCo/Al_2O_3 catalysts: (a) Fresh; (b) reduced at 400 °C. (●) Co_3O_4, (▲) CoO, and (△) Co^0.

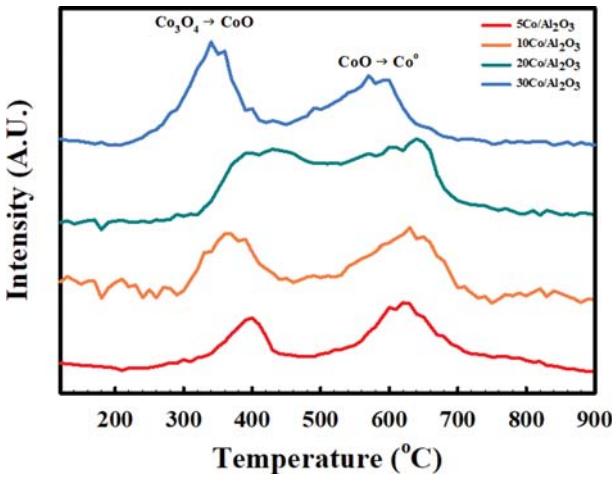

Fig. 3. H_2-TPR profiles of the xCo/Al_2O_3 catalysts.

The reduction of the Al_2O_3-supported Co catalysts was measured by H_2-TPR experiments, which were performed under 10 vol% H_2/N_2 flow at a heating rate of 10 °C/min. The reduction profiles of the Co/Al_2O_3 catalysts in Fig. 3 indicated two distinct reduction peaks. The first peak centered at 400 °C was ascribed to the transformation of Co_3O_4 to CoO, while the second peak at 620 °C could be attributed to the transformation of CoO to Co^0. In addition, the second reduction peak shifted to lower temperatures as the Co loading increased, resulting in overlapping of the two peaks in the profile of $20Co/Al_2O_3$. This result also indicated that a high Co loading promoted the reduction of CoO to Co^0 due to the large crystallite size in the Co phase, which in turn led to a higher percentage of CO conversion. Indeed, the degree of reduction increased from 50.0% to 72.3% with increasing Co loading (Table 1). However, the selectivity for C_2-C_4 hydrocarbons dropped sharply as Co loading increased.

2. Co/SiO_2 Catalysts for CO Hydrogenation

The catalytic performance of the SiO_2-supported Co catalysts was studied for the production of C_2-C_4 hydrocarbons with high CO conversion. Due to the weak interactions between Co and the SiO_2 surface, the SiO_2 support would enable a more facile Co reduction than the Al_2O_3 support [18,19,23]. Based on the physicochemical properties of the SiO_2-supported catalysts (Table 2), as the Co loading increased from 0 to 30 wt%, the BET surface area and the pore volume dropped from 305.9 to 180.0 m^2/g and from 1.03 to 0.55 cm^3/g, respectively. Moreover, the average pore size in the Co/SiO_2 catalysts did not change after impregnation with Co (Fig. S2).

The XRD patterns of the calcined Co/SiO_2 catalysts (Fig. 4) confirmed the presence of the Co_3O_4 phase on SiO_2. The Co_3O_4 crystallites in the SiO_2-supported catalysts were larger than those in the Al_2O_3-supported catalysts with equal Co loadings (Table 2) due to the weak interactions between the metal and the surface of the SiO_2 support. In addition, clear Co^0 diffraction peaks were observed at 44.5° in the patterns of the reduced Co/SiO_2 catalysts, while no CoO peaks were identified. Consequently, the SiO_2-supported catalysts resulted in greater Co reduction than the Al_2O_3-supported cata-

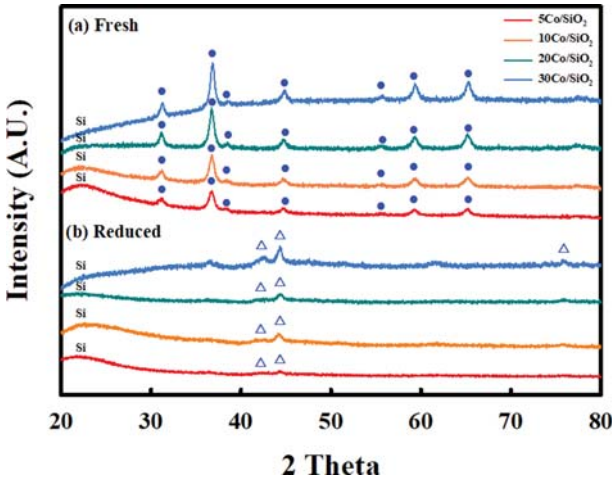

Fig. 4. XRD patterns of the *x*Co/SiO_2 catalysts: (a) fresh; (b) reduced at 400 °C. (●) Co_3O_4, (▲) CoO, and (△) Co^0.

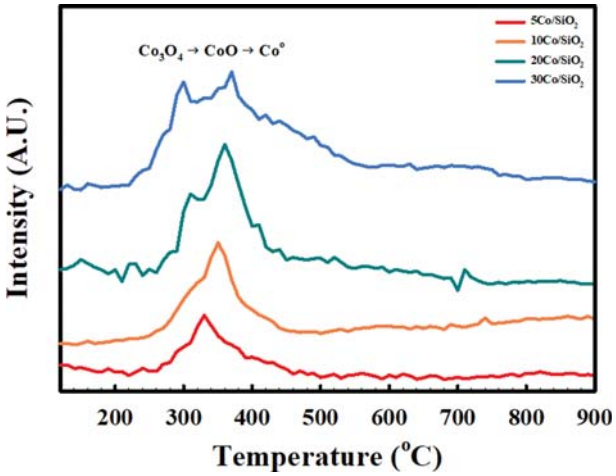

Fig. 5. H_2-TPR profiles of the *x*Co/SiO_2 catalysts.

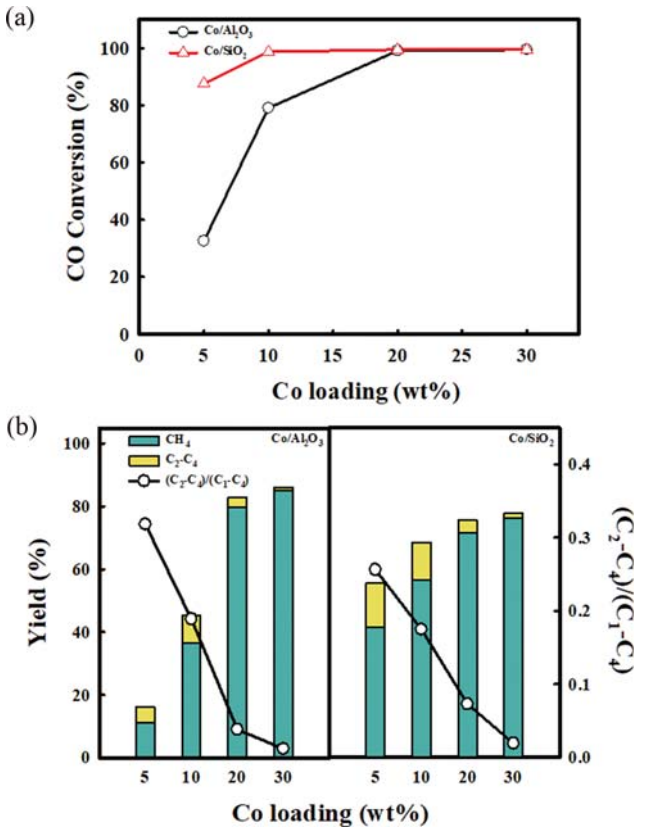

Fig. 6. (a) CO conversion over the Co/SiO_2 and Co/Al_2O_3 catalysts with different Co loading; (b) selectivity of CH_4 and C_2-C_4, and (C_2-C_4)/(C_1-C_4) ratios of the Co/SiO_2 and Co/Al_2O_3 catalysts with different Co loading.

lysts due to the weak interactions between the metal and the support, as also determined by the calculated reducibility of the Co/Al_2O_3 and Co/SiO_2 catalysts.

The reduction of the SiO_2-supported CoO catalysts was evaluated by H_2-TPR experiments. In particular, broad peaks centered at 350 °C were observed in the reduction profiles of the Co/SiO_2 catalysts (Fig. 5), which represented the reduction of Co_3O_4 to CoO and that of CoO to Co^0. The reduction temperature of CoO to Co^0 in the SiO_2-supported catalysts was significantly lower than that in the Al_2O_3-supported catalysts (Fig. 3), also due to the weak interactions between SiO_2 and the Co metal [19].

The CO conversion was performed using an H_2/CO ratio of 3.0 at 300 °C and 10 bar after reduction at 400 °C. Based on the data of Fig. 6(a) and Table 3, the percentage of CO conversion was higher over Co/SiO_2 than over the Co/Al_2O_3 catalysts with equal Co loadings. More specifically, the CO conversion was 87.6% over the SiO_2-supported catalyst that contained 5 wt% Co, whereas the corresponding value over the Al_2O_3-supported catalyst was much lower: 32.6%. The CO conversion increased over both catalysts when the Co loading was increased to 10 wt%. However, the percentage of CO conversion over 10Co/SiO_2 was 98.7%, whereas a CO conversion of only 79.1% was obtained with the 10Co/Al_2O_3 catalyst. Furthermore, the maximum CO conversion over the SiO_2- and Al_2O_3-supported catalysts was achieved with a Co loading of 20 wt%. Interestingly, the CO conversion was remarkably high (87.6%) over the SiO_2-supported catalysts, even at a Co loading of 5 wt%, because Co_3O_4 was completely reduced to Co^0 on the SiO_2 support in contrast to the Al_2O_3 support. In addition, the TOF value decreased with increasing Co loading over the Co/SiO_2 catalysts, because the CO conversion of the 5-30Co/SiO_2 catalysts was very high (>87.6%, Table 3, Fig. S4). Thus, the TOF value for Co/SiO_2 catalysts was inaccurate under these conditions.

The change in the yields of the light C_1-C_4 hydrocarbons and the ratios of the C_2-C_4 to C_1-C_4 hydrocarbons was explored as a function of the Co loading (Fig. 6(b)). The sum of the CH_4 and C_2-C_4 yields increased from 16% to 86% as the Co loading in the Co/Al_2O_3 catalysts increased from 5 to 30 wt%, while the (C_2-C_4)/(C_1-C_4) ratio decreased from 0.32 to 0.01. The sum of the CH_4 and C_2-C_4 yields increased from 56% to 78% as the Co loading in the Co/SiO_2 catalysts increased from 5 wt% to 30 wt%, whereas the (C_2-C_4)/(C_1-C_4) ratio decreased from 0.25 to 0.03. These results indicated that increasing the Co loading increased the CH_4 yield and reduced the C_2-C_4 yield. Moreover, the increase in the com-

Table 3. Performance of the Al_2O_3- and SiO_2-supported Co catalysts as a function of Co loading

Catalyst	CO conversion (%)	Selectivity (%)								TOF[a] (10^{-2} s^{-1})
		CH_4	C_2-C_4					C_{5+}	CO_2	
			C_2H_6	C_2H_4	C_3H_8	C_3H_6	C_4H_{10}	C_4H_8		
5Co/Al_2O_3	32.6	33.8	15.8						49.6	0.8	0.23
			3.9	0.0	3.3	5.7	2.9	0.0			
10Co/Al_2O_3	79.1	46.3	10.8						32.5	10.4	0.26
			5.1	0.0	3.4	0.5	1.7	0.1			
20Co/Al_2O_3	99.1	80.5	3.2						4.5	11.8	0.20
			2.4	0.0	0.8	0.0	0.0	0.0			
30Co/Al_2O_3	99.5	85.8	1.1						0.0	13.1	0.21
			1.1	0.0	0.0	0.0	0.0	0.0			
5Co/SiO_2	87.6	47.3	16.3						21.1	15.3	0.58
			6.6	0.0	6.0	0.0	3.7	0.0			
10Co/SiO_2	98.7	58.1	12.3						9.4	20.2	0.29
			6.0	0.0	4.2	0.0	2.0	0.0			
20Co/SiO_2	99.5	71.8	4.2						4.0	20.1	0.17
			3.3	0.0	0.9	0.0	0.0	0.0			
30Co/SiO_2	99.5	76.8	2.0						0.0	21.2	0.11
			1.5	0.0	0.5	0.0	0.0	0.0			

[a]Calculated based on the mole of CO converted per mole of surface Co per s: TOF=(GHSV×24%/22.4×CO conversion)/active metal content/reaction time.

bined yields of CH_4 and C_2-C_4 obtained over the Co/Al_2O_3 catalysts was remarkably different from that obtained over the Co/SiO_2 catalysts, due to the increase in the CO conversion. Overall, the increase in the Co loading from 5 to 30 wt% increased the yield of light hydrocarbons in the C_1-C_4 range, taking into account that the increased number of active Co sites can enhance the methanation reaction [27]. In addition, the C_2-C_4 to C_1-C_4 ratio decreased due to the significant increase in the CH_4 yields and the decrease in the C_2-C_4 yield.

3. Effect of Reduction Temperature on the Al_2O_3- and SiO_2-Supported Catalysts

The effect of the reduction conditions on the performance of the Co-based catalysts for HC-SNG production was also examined. The XRD patterns of the 10Co/Al_2O_3 and 10Co/SiO_2 catalysts were obtained after reduction at 400 °C, 500 °C, and 600 °C for 1 h in 10 vol% H_2/N_2 at a flow rate of 100 mL/min (Fig. 7). The diffraction peaks of the crystalline Co^0 could be clearly detected in the patterns of the reduced Co/Al_2O_3 catalysts, and the peak intensities increased with increasing reduction temperature. Clear Co^0 peaks could also be detected in the patterns of the SiO_2-supported catalysts reduced at 400 °C, 500 °C, and 600 °C, suggesting that the Co/SiO_2 catalysts could be completely reduced at 400 °C, while the Co phase in the Co/Al_2O_3 catalysts was partially reduced at the same reduction temperature.

The influence of the reduction temperature on the catalytic performance of the Co/Al_2O_3 and Co/SiO_2 catalysts is graphically presented in Fig. 8 and the corresponding results are summarized in Table 4. The percentage of the CO conversion over the 10Co/Al_2O_3 catalyst increased remarkably from 79.1% to 99.9% when the reduction temperature increased from 400 °C to 500 °C. The enhancement of the CO conversion was attributed to the greater Co reduction at 500 °C, although the CO conversion was slightly lower after the catalyst reduction at 600 °C. In contrast, the CO conversion over the 10Co/SiO_2 catalyst gradually decreased from 98.7% to 87.6% as the reduction temperature increased from 400 °C to 600 °C. This result demonstrated that the size of the Co^0 crystallites in the SiO_2-supported catalyst increased with the reduction temperature (Table S1), which in turn reduced the number of active sites available for reaction. The CH_4 selectivity of the 10Co/Al_2O_3 catalyst increased from 46.3% after reduction at 400 °C to 66.2% after reduction at 500 °C. Its selectivity for C_2-C_4 hydrocarbons also increased from 10.8% after reduction at 400 °C to 14.3% after reduction at 600 °C, but its C_{5+} selectivity decreased from 32.5% to 9.2% with increasing reduction temperature. However, the CH_4 and C_{5+} selectivities of the 10Co/SiO_2 catalyst were different from those of the Co/Al_2O_3 catalyst. In particular, the CH_4 selectivity of the 10Co/SiO_2 catalyst decreased from 58.1% after reduction at 400 °C to 40.0% after reduction at 600 °C, whereas its selectivity values for C_2-C_4 and C_{5+} increased from 12.3% and 9.4% to 16.3% and 30.7%, respectively. It is also known that larger Co crystallites afford high yields of long-chain hydrocarbons in traditional FTS [28-31]. Therefore, the high CO conversion and C_2-C_4 selectivity of the 10Co/SiO_2 catalyst may be related to the reducibility of the Co oxide.

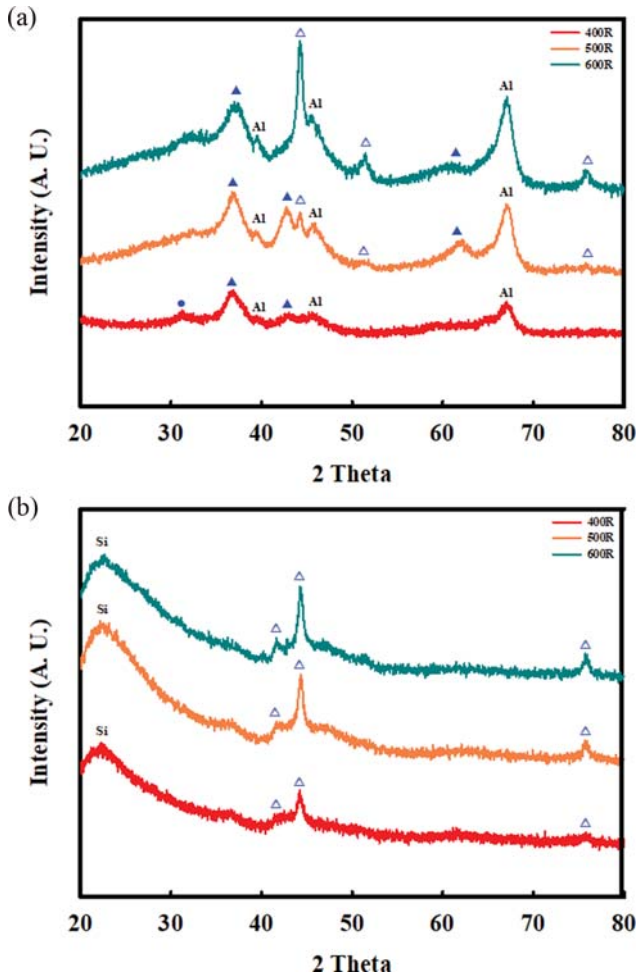

Fig. 7. XRD patterns of the catalysts after reduction at 400 °C, 500 °C, and 600 °C. (a) $10Co/Al_2O_3$; (b) $10Co/SiO_2$. (●) Co_3O_4, (▲) CoO, and (△) Co^0.

4. Co/Al_2O_3 and Co/SiO_2 Product Gas Heating Values

The heating values of the HC-SNG product gases generated over the $10Co/Al_2O_3$ and $10Co/SiO_2$ catalysts after reduction at

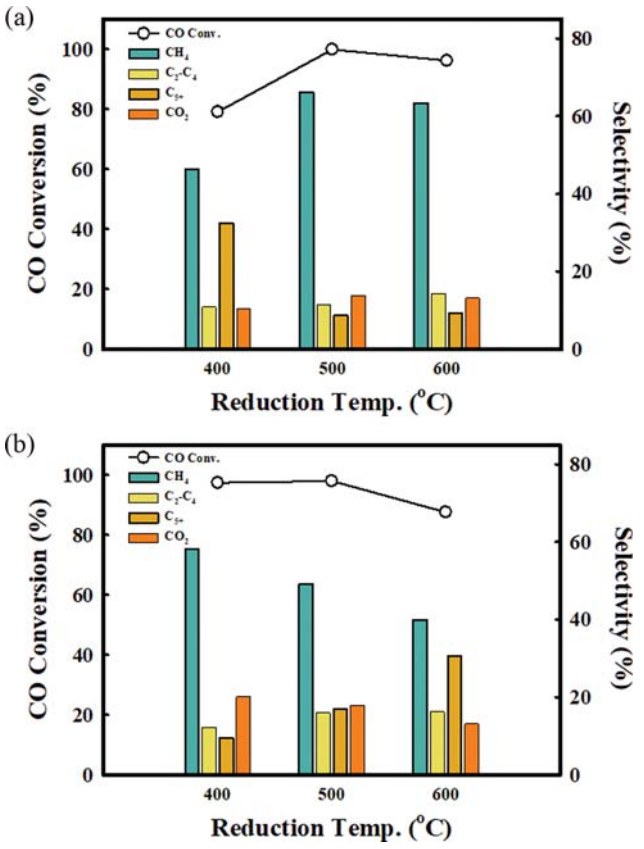

Fig. 8. CO conversion over the (a) Co/Al_2O_3 and (b) Co/SiO_2 catalysts and selectivity for CH_4, C_2-C_4, C_{5+}, and CO_2 as a function of reduction temperature.

Table 4. Performance of the Al_2O_3- and SiO_2-supported Co catalysts as a function of the reduction temperature

Catalyst	Reduction temperature (°C)	CO conversion (%)	Selectivity (%)								
			CH_4	C_2-C_4					C_{5+}	CO_2
				C_2H_6	C_2H_4	C_3H_8	C_3H_6	C_4H_{10}	C_4H_8		
$10Co/Al_2O_3$	400	79.1	46.3	10.8						32.5	10.4
				5.1	0.0	3.4	0.5	1.7	0.1		
	500	99.9	66.2	11.4						8.6	13.8
				5.4	0.0	3.9	0.0	2.1	0.0		
	600	96.2	63.4	14.3						9.2	13.1
				6.8	0.0	5.0	0.0	2.5	0.0		
$10Co/SiO_2$	400	98.7	58.1	12.3						9.4	20.2
				6.0	0.0	4.2	0.0	2.0	0.0		
	500	98.0	49.1	16.0						17.1	17.9
				6.3	0.0	6.0	0.0	3.6	0.0		
	600	87.6	40.0	16.3						30.7	13.1
				5.6	0.0	5.5	1.5	3.6	0.0		

Table 5. Heating values of the product gases obtained over the Al_2O_3- and SiO_2-supported Co catalysts based on the volumetric fractions of various hydrocarbons after 10 h

Catalyst	Reduction temperature (°C)	CO conversion (%)	Volume fractions (%)				Heating value (kcal/Nm^3)
			CH_4	C_2H_6	C_3H_8	C_4H_{10}	
$10Co/Al_2O_3$	400	79.1±0.5	91.5±1.0	5.0±0.2	2.6±0.1	0.8±0.1	10,457
	500	99.9±0.2	93.6±0.2	3.8±0.4	1.8±0.2	0.7±0.1	10,238
	600	96.2±0.8	91.8±0.6	4.9±0.2	2.4±0.1	0.9±0.3	10,439
$10Co/SiO_2$	400	98.7±0.5	92.2±0.3	4.8±0.1	2.2±0.1	0.8±0.3	10,405
	500	98.4±0.4	89.0±0.4	5.7±0.2	3.6±0.1	1.2±0.1	10,839
	600	87.6±0.8	85.0±0.4	6.0±0.2	7.1±0.2	1.9±0.1	11,150
$10Co\text{-}6Mn\text{-}2.5Ru/Al_2O_3$	400	99.9	87.2	5.5	4.5	2.6	11,192
$20Co\text{-}16Mn/Al_2O_3$	700	99.9	85.4	7.2	5.4	1.9	11,278
Heating value of pure gas (kcal/Nm^3)			9,523	16,814	24,179	32,059	

different temperatures were also estimated (Table 5). The CO conversion and the hydrocarbon selectivity of the catalysts did not drastically change after 10 h on the reaction stream, as shown in Fig. S3. The heating value of each product gas was determined from the volumetric hydrocarbon fraction by calculating the heating values of the pure gases in the C_1-C_4 hydrocarbon range in the outlet gas. N_2, H_2, CO, and CO_2 were excluded from the calculations. Thus, the CO conversion over the $10Co/SiO_2$ catalyst was high after reduction at 400 °C, and the heating value of the product gas was 10,405 kcal/Nm^3. Therefore, even without a high reduction temperature (700 °C) or a noble metal (Ru), the heating value of the product gas exceeded the standard heating value for power generation, implying the possibility of increasing the heating value of natural gas without adding LPG.

CONCLUSIONS

The catalytic performance of Co-based catalysts developed on Al_2O_3 and SiO_2 supports was investigated for the production of HC-SNG. The percentage of CO conversion over the Co/SiO_2 catalysts was higher than that over Co/Al_2O_3, mainly due to the weak interactions between the Co species and the SiO_2 surface, which facilitated the reduction of Co species, as confirmed by XRD analysis and H_2-TPR. Increasing the Co loading in the catalysts led to enhanced reduction of CoO to Co^0. Moreover, the Co_3O_4 crystallites in the Co/SiO_2 catalysts were larger than those in the Co/Al_2O_3 catalysts, while the crystallite size increased with increasing reduction temperature. The optimum performance of the Co/SiO_2 catalysts was achieved after reduction at 400 °C. However, the C_2-C_4 selectivity decreased sharply as the Co loading increased. Investigation of the effect of the reduction temperature on the performance of the Co/Al_2O_3 and Co/SiO_2 catalysts indicated that the temperature of Co/Al_2O_3 reduction led to a remarkable increase in CO conversion, because Co in the Co_3O_4 phase of Co/Al_2O_3 was not reduced to Co^0 at 400 °C. Increasing the reduction temperature of the Co/SiO_2 catalysts led to a decrease in CO conversion due to metal sintering at high temperature. Thus, the CO conversion was mainly affected by the reduction of Co species and metal sintering. The product gas obtained over the $10Co/SiO_2$ catalyst after reduction at 400 °C satisfied the standard heating value and was achieved without a high reduction temperature (700 °C) or a noble metal (Ru).

ACKNOWLEDGEMENTS

This work was supported by the Korea Institute of Energy Technology Evaluation and Planning (KETEP) and the Ministry of Trade, Industry & Energy (MOTIE) of the Republic of Korea (20183010032400).

SUPPORTING INFORMATION

Additional information as noted in the text. This information is available via the Internet at http://www.springer.com/chemistry/journal/11814.

REFERENCES

1. S. J. Davis, K. Caldeira and H. D. Matthews, *Science*, **329**, 1330 (2010).
2. S. B. Jo, H. J. Chae, T. Y. Kim, C. H. Lee, J. U. Oh, S.-H. Kang, J. W. Kim, M. Jeong, S. C. Lee and J. C. Kim, *Catal. Commun.*, **117**, 74 (2018).
3. Y. H. Lee, H. Kim, H. S. Choi, D.-W. Lee and K.-Y. Lee, *Korean J. Chem. Eng.*, **32**, 2220 (2015).
4. Y. H. Lee, D.-W. Lee and K.-Y. Lee, *J. Mol. Catal. A-Chem.*, **425**, 190 (2016).
5. I. Czekaj, F. Loviat, F. Raimondi, J. Wambach, S. Biollaz and A. Wokaun, *Appl. Catal. A-Gen.*, **329**, 68 (2007).
6. C. Guo, Y. Wu, H. Qin and J. Zhang, *Fuel Process. Technol.*, **124**, 61 (2014).
7. D. Hu, J. Gao, Y. Ping, L. Jia, P. Gunawan, Z. Zhong, G. Xu, F. Gu and F. Su, *Ind. Eng. Chem. Res.*, **51**, 4875 (2012).
8. K. B. Kester, E. Zagli and J. L. Falconer, *Appl. Catal.*, **22**, 311 (1986).
9. J. Sehested, S. Dahl, J. Jacobsen and J. R. Rostrup-Nielsen, *J. Phys. Chem. B*, **109**, 2432 (2005).

10. J. Kopyscinski, T. J. Schildhauer and S. M. Biollaz, *Fuel*, **89**, 1763 (2010).
11. S. Rönsch, J. Schneider, S. Matthischke, M. Schlüter, M. Götz, J. Lefebvre, P. Prabhakaran and S. Bajohr, *Fuel*, **166**, 276 (2016).
12. B. H. Davis, *Ind. Eng. Chem. Res.*, **46**, 8938 (2007).
13. J. Den Breejen, P. Radstake, G. Bezemer, J. Bitter, V. Frøseth, A. Holmen and K. P. de Jong, *J. Am. Chem. Soc.*, **131**, 7197 (2009).
14. Z.-j. Wang, Z. Yan, C.-j. Liu and D. Goodman, *ChemCatChem*, **3**, 551 (2011).
15. C. Weststrate, J. Van De Loosdrecht and J. Niemantsverdriet, *J. Catal.*, **342**, 1 (2016).
16. T. Inui, A. Sakamoto, T. Takeguchi and Y. Ishigaki, *Ind. Eng. Chem. Res.*, **28**, 427 (1989).
17. Y. Ishigaki, M. Uba, S. Nishida and T. Inui, *Appl. Catal.*, **47**, 197 (1989).
18. J.-H. Oh, J. W. Bae, S.-J. Park, P. Khanna and K.-W. Jun, *Catal. Lett.*, **130**, 403 (2009).
19. K. S. Park, K. Saravanan, S.-J. Park, Y.-J. Lee, K.-W. Jeon and J. W. Bae, *Catal. Sci. Technol.*, **7**, 4079 (2017).
20. R. C. Reuel and C. H. Bartholomew, *J. Catal.*, **85**, 78 (1984).
21. H. G. Salazar-Contreras, A. Martínez-Hernández, A. A. Boix, G. A. Fuentes and E. Torres-García, *Appl. Catal. B-Environ.*, **244**, 414 (2019).
22. J. Zhang, J. Chen, J. Ren and Y. Sun, *Appl. Catal. A-Gen.*, **243**, 121 (2003).
23. Y. Zhang, S. Nagamori, S. Hinchiranan, T. Vitidsant and N. Tsubaki, *Energy Fuel*, **20**, 417 (2006).
24. G. T. Armstrong and T. L. Jobe Jr., *Heating values of natural gas and its components*, U.S. Department of Commerce, Washington, D.C. (1982).
25. H. M. Torres Galvis and K. P. de Jong, *ACS Catal.*, **3**, 2130 (2013).
26. W. Li, X. Nie, X. Jiang, A. Zhang, F. Ding, M. Liu, Z. Liu, X. Guo and C. Song, *Appl. Catal. B-Environ.*, **220**, 397 (2018).
27. S. Ullah, E. C. Lovell, R. J. Wong, T. H. Tan, J. Scott and R. Amal, *ACS Sustain. Chem. Eng.*, **8**, 5056 (2020).
28. W.-P. Ma, Y.-J. Ding and L.-W. Lin, *Ind. Eng. Chem. Res.*, **43**, 2391 (2004).
29. A. Y. Khodakov, R. Bechara and A. Griboval-Constant, *Appl. Catal. A-Gen.*, **254**, 273 (2003).
30. A. Martínez, C. López, F. Márquez and I. Díaz, *J. Catal.*, **220**, 486 (2003).
31. C. Medina, R. García, P. Reyes, J. Fierro and N. Escalona, *Appl. Catal. A-Gen.*, **373**, 71 (2010).

Supporting Information

Effect of reducibility on the performance of Co-based catalysts for the production of high-calorie synthetic natural gas

Tae Young Kim*,‡, Seong Bin Jo,‡, Chul Ho Lee***, Suk-Hwan Kang****, Joon Woo Kim*****, Soo Chool Lee**,†, and Jae Chang Kim*,†**

*Department of Chemical Engineering, Kyungpook National University, Daegu 41566, Korea
**Research Institute of Advanced Energy Technology, Kyungpook National University, Daegu 41566, Korea
***Korea Institute of Industrial Technology, Ulsan 44413, Korea
****Institute for Advanced Engineering, Yongin 41718, Korea
*****Research Institute of Industrial Science and Technology, Pohang 37673, Korea
(*Received 20 February 2020 • Revised 20 May 2020 • Accepted 27 May 2020*)

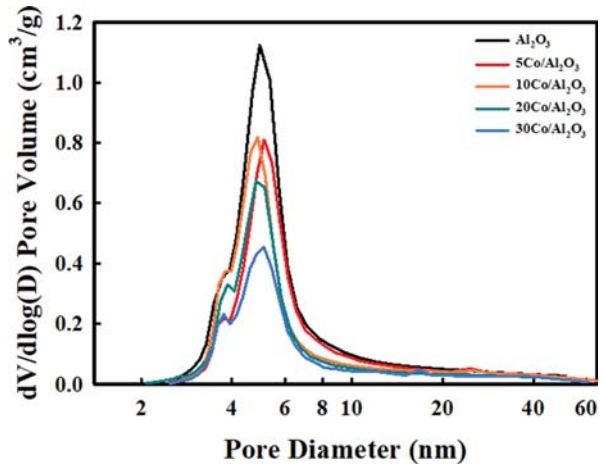

Fig. S1. BJH pore size distribution curves, calculated from nitrogen desorption isotherms for the Al_2O_3 support and *x*Co/Al_2O_3 catalysts.

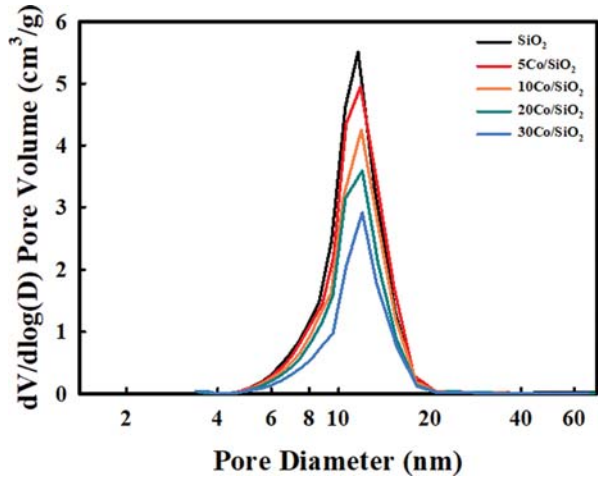

Fig. S2. BJH pore size distribution curves, calculated from nitrogen desorption isotherms for the SiO_2 support and *x*Co/SiO_2 catalysts.

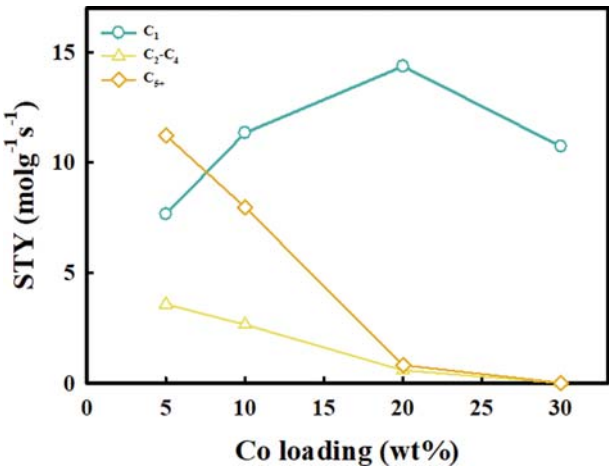

Fig. S3. The STY of CH_4, C_2-C_4 and C_{5+} over the *x*Co/Al_2O_3 catalysts.

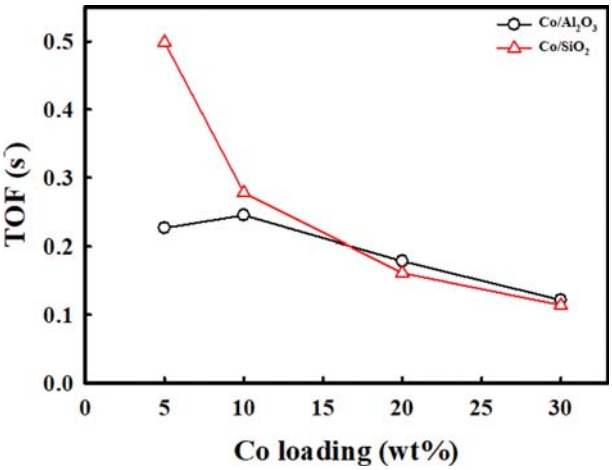

Fig. S4. TOF of CO conversion as function of Co loadings on Co/Al_2O_3 and Co/SiO_2 catalysts.

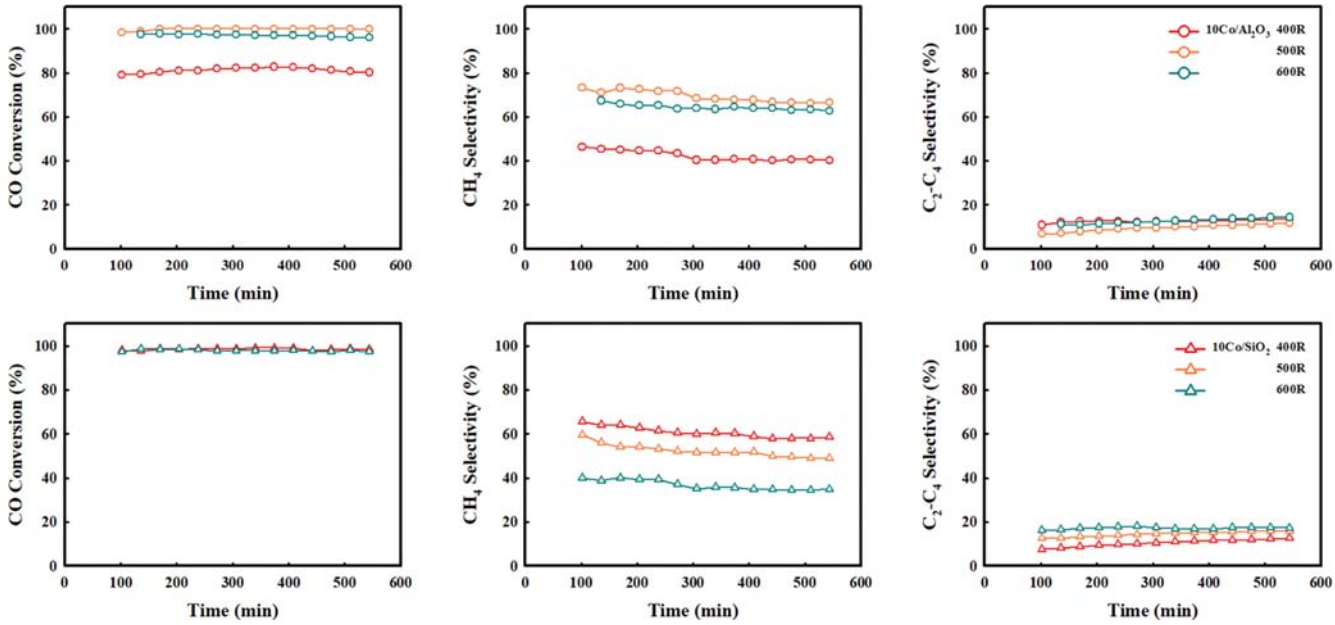

Fig. S5. Time on stream profiles of CO conversion and hydrocarbon selectivity over the Al_2O_3- and SiO_2-supported cobalt catalysts as a function of reduction temperature.

Table S1. The catalytic performance of Al_2O_3 and SiO_2-supported cobalt catalysts as a function of cobalt loading

	Reduction temperature (°C)	XRD crystallite size (nm)		
		Fresh Co_3O_4	Reduced	
			CoO	Co^0
$10Co/Al_2O_3$	400	8.8	6.9	-
	500		7.7	4.3
	600		-	10.8
$10Co/SiO_2$	400	12.9	-	8.0
	500		-	9.0
	600		-	10.1